COMPDYN 2011
3rd ECCOMAS Thematic Conference on
Computational Methods in Structural Dynamics and Earthquake Engineering
M. Papadrakakis, M. Fragiadakis, V. Plevris (eds.)
Corfu, Greece, 25-28 May 2011

MODEL UNCERTAINTIES IN SMART STRUCTURES

Amalia J. Moutsopoulou[1], Georgios E. Stavroulakis[2], and Anastasios T. Pouliezos[2]

[1]Department of Civil Engineering, Technological Educational Institute of Crete
Estavromenos, 71004, Heraklion
e-mail: amalia@staff.teicrete.gr

[2] Department of Production Engineering and Management, Technical University of Crete
Kounoupidiana, 73100, Chania
e-mail: gestavr@dpem.tuc.gr, tasos@dpem.tuc.gr

Keywords: Uncertainty, Smart beam, Strochastic load, Robust performance, Robust analysis, Robust synthesis.

Abstract. *This paper deals with the incorporation of model uncertainties and the usage of robust control techniques in active vibration suppression of smart structures. The used advanced control techniques are based on the H_∞ criterion and m-analysis. Both techniques allow us to take into account the worst case scenario of uncertain disturbances and noise of the system. The presented results demonstrate remarkable efficiency of the proposed techniques.*

1 INTRODUCTION

The field of smart structures has been an emerging area of research for the last few decades [2, 3, 4, 5, 9]. Smart structures are equipped with sensors, actuators and controlunits, and are able to respond in a smart way to external stimuli. The importance of this field is supported by developments in the field of materials science and technology and in the fiels of control and electronics. In materials science, new smart materials are developed that can be used for sensing and actuation in an efficient and controlled manner. These smart materials can be integrated into structures so they can be employed as actuators and sensors for the resulting smart composite structure. On the other hand the applicability of a smart structure strongly depends on the efficient design and implementation of the control systems. Critical issues, like deviation of the structure or the environment from their nominal values or time-delay, must be addressed. In this paper we focus our attention on the existence of uncertainties in smart structures. A finite element based model of a smart beam equipped with uncertainties is used. Based on this model an H_∞ and a μ-controller are designed which effectively suppress the vibrations of the smart beam under stochastic wind-type loading. The advantage of the H_∞ criterion is its ability to take into account the worst influence of uncertain disturbances or noise in the system. By using this technique it is possible to synthesize a H_∞ controller which will be robust with respect to a prespecified number of errors in the model.

Uncertainties in a structural model may arise from non-linearities which are not taken into account in a linear model, from inaccurate knowledge of certain parameters (for example, damping), from unmodelled dynamics in higher frequencies, as well as from their variations over the life of the structure. On the structural model with uncertainties a robust μ-controller is analyzed and synthesized, using the $D-K$ iterative method. The results are compared and commented upon using the various controllers. The results are very good: the oscillations were suppressed even for a real aeolian load, with the required voltages of the piezoelectric components taking values within their endurance limits.

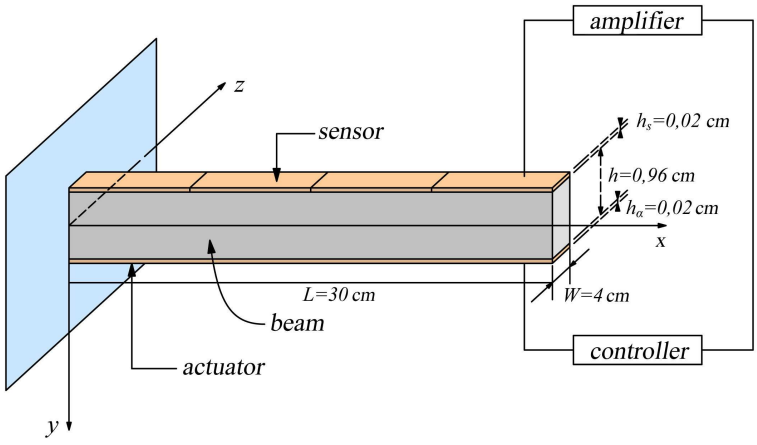

Figure 1: Beam with piezoelectric sensors/actuators.

2 MATHEMATICAL MODELLING

A cantilever slender beam with rectangular cross-section is considered. Four pairs of piezoelectric patches are embedded symmetrically at the top and the bottom surfaces of the beam,

as shown in Fig. 1. The beam is made from graphite- epoxy $T300-976$ and the piezoelectric patches are $PZTG1195N$. The top patches act like sensors and the bottom like actuators. The resulting composite beam is modelled by means of the classical laminated technical theory of bending. Furthermore, we assume that the mechanical properties of both the piezoelectric material and the host beam are independent in time. The thermal effects are considered to be negligible as well [9].

The beam has length L, width b and thickness h. The sensors and the actuators have width b_S and b_A and thickness h_S and h_A, respectively. The electromechanical parameters of the beam used for the application of the method in this paper are given in the table.

Parameters	Values
Beam length, L	$0.3m$
Beam width, W	$0.04m$
Beam thickness, h	$0.0096m$
Beam density, ρ	$1600kg/m$
Youngs modulus of the beam, E	$1.5\times10^{11}N/m^2$
Piezoelectric constant, d_{31}	$254\times10^{-12}m/V$
Electric constant, ξ_{33}	$11.5\times10^{-3}Vm/N$
Young's modulus of the piezoelectric element	$1.5\times10^{11}N/m^2$
Width of the piezoelectric element	$b_S=b_a=0.04m$
Thickness of the piezoelectric element	$h_S=h_a=0.0002m$

Table 1: Parameters of the composite beam.

2.1 Piezoelectric equations

In order to derive the basic equations for piezoelectric sensors and actuators (S/As), we assume that:

- The piezoelectric S/A are bonded perfectly on the host beam;
- The piezoelectric layers are much thinner then the host beam;
- The piezoelectric material is homogeneous, transversely isotropic and linearly elastic;
- The piezoelectric S/A are transversely polarized (in the z-direction)[9].

Under these assumptions the three-dimensional linear constitutive equations are given by [8],

$$\left\{ \begin{array}{c} \sigma_{xx} \\ \sigma_{xz} \end{array} \right\} = \left[\begin{array}{cc} Q_{11} & 0 \\ 0 & Q_{55} \end{array} \right] \left(\left\{ \begin{array}{c} \varepsilon_{xx} \\ \varepsilon_{xz} \end{array} \right\} - \left[\begin{array}{c} d_{31} \\ 0 \end{array} \right] E_z \right) \tag{1}$$

$$D_z = Q_{11} d_{31} \varepsilon_{xx} + \xi_{xx} E_z \tag{2}$$

where σ_{xx}, σ_{xz} denote the axial and shear stress components, D_z, denotes the transverse electrical displacement; ε_{xx} and ε_{xz} are axial and shear strain components; Q_{11}, and Q_{55}, denote

elastic constants; d_{31}, and ξ_{33}, denote piezoelectric and dielectric constants, respectively. Equation 1 describes the inverse piezoelectric effect and equation 2 describes the direct piezoelectric effect. E_z, is the transverse component of the electric field that is assumed to be constant for the piezoelectric layers and its components in the xy-plain are supposed to vanish. If no electric field is applied in the sensor layer, the direct piezoelectric equation 2 is fermed like this,

$$D_z = Q_{11} d_{31} \varepsilon_{xx} \tag{3}$$

and it is used to calculate the output charge created by the strains in the beam.[7]

2.2 Equations of motion

We assume that:

- The beam centroidal and elastic axis coincides with the x-coordinate axis so that no bending-torsion coupling is considered;
- The axial vibration of the host beam is considered negligible;
- The displacement field $\{u\} = (u_1, u_2, u_3)$ is obtained based on the usual Timoshenko assumptions [1],

$$\begin{aligned} u_1(x,y,z) &\approx z\phi(x,t) \\ u_2(x,y,z) &\approx 0 \\ u_3(x,y,x) &\approx \mathbf{w}(x,t) \end{aligned} \tag{4}$$

where ϕ is the rotation of the beam's cross-section about the positive y-axis and w is the transverse displacement of a point of the centroidal axis $(y = z = 0)$.
The strain displacement relations can be applied to equation 4 to give,

$$\varepsilon_{xx} = z\frac{\vartheta\phi}{\vartheta x} \quad \varepsilon_{xz} = \phi + \frac{\vartheta \mathbf{w}}{\vartheta x} \tag{5}$$

We suppose that the transverse shear deformation ε_{xx} is equal to zero[2].
In order to derive the equations of the motion of the beam we use Hamilton's principle,[11]

$$\int_{t_2}^{t_1} (\delta T - \delta U + \delta W) dt = 0, \tag{6}$$

where T is the total kinetic energy of the system, U is the potential (strain) energy and W is the virtual work done by the external mechanical and electrical loads and moments. The first variation of the kinetic energy is given by,

$$\begin{aligned} \delta T &= \frac{1}{2}\int_V \rho \left\{\frac{\vartheta u}{\vartheta t}\right\}^r \left\{\frac{\vartheta u}{\vartheta t}\right\} dV \\ &= \frac{b}{2}\int_0^L \int_{-\frac{h}{2}-h_a}^{\frac{h}{2}+h_s} \rho \left(z\frac{\vartheta\phi}{\vartheta t}\delta\frac{\vartheta\phi}{\vartheta t} + \frac{\vartheta \mathbf{w}}{\vartheta t}\delta\frac{\vartheta \mathbf{w}}{\vartheta t}\right) dz dx \end{aligned} \tag{7}$$

The first variation of the kinetic energy is given by,

$$\begin{aligned} \delta U &= \frac{1}{2}\int_V \delta\{\epsilon\}^T\{\sigma\}dV \\ &= \frac{b}{2}\int_0^L \int_{-\frac{h}{2}-h_a}^{\frac{h}{2}+h_s} \left[Q_{11}\left(z\frac{\vartheta \mathbf{w}}{\vartheta x}\delta\right)\left(z\frac{\vartheta \mathbf{w}}{\vartheta x}\right)\right] dzdx \end{aligned} \tag{8}$$

If the load consists only of moments induced by piezoelectric actuators and since the structure has no bending twisting couple then the first variation of the work has the form [11],

$$\delta W = b\int_0^L M^a \delta\left(\frac{\vartheta\phi}{\vartheta x}\right) dx \tag{9}$$

where M^a is the moment per unit length induced by the actuator layer and is given by,

$$\begin{aligned} M^a = \int_{-\frac{h}{2}-h_a}^{-\frac{h}{2}} z\sigma_{xx}^a dz \;\; &= \int_{-\frac{h}{2}-h_a}^{-\frac{h}{2}} zQ_{11}d_{31}E_z^a dz \\ &\left(E_z^a = \frac{V_a}{h_a}\right) \end{aligned} \tag{10}$$

2.3 Finite element formulation

We consider a beam element of length L_e, which has two mechanical degrees of freedom at each node: one translational ω_1 (respectively ω_2) in direction y and one rotational ψ_1 (respectively ψ_2), as it is shown in Fig. 2. The vector of nodal displacements and rotations q_e is defined

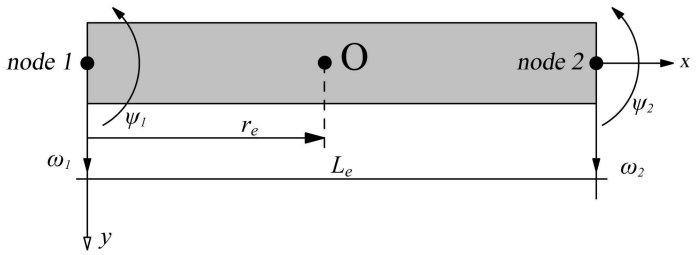

Figure 2: Beam finite element.

as [8],

$$q_e = [\omega_1, \psi_1, \omega_2, \psi_2] \tag{11}$$

The transverse deflection $\omega(x,t)$ and rotation $\psi(x,t)$ along the beam are continuous and they are interpolated by Hermitian linear shape functions H_i^ω and H_i^ψ as follows[5],

$$\begin{aligned} \omega(x,t) &= \sum_{i=1}^{4} H_i^\omega(x) q_i(t) \\ \psi(x,t) &= \sum_{i=1}^{4} H_i^\psi(x) q_i(t) \end{aligned} \tag{12}$$

This classical finite element procedure leads to the approximate (discretized) problem. For a finite element the discrete differential equations are obtained by substituting the discretized expressions 13 into equations 8 and 9 to evaluate the kinetic and strain energies. Integrating over spatial domains and using the Hamilton's principle 6 the equation of motion for a beam element are expressed in terms of nodal variable q as follows [2, 6, 8],

$$M\ddot{q}(t) + D\dot{q}(t) + Kq(t) = f_m(t) + f_e(t) \tag{13}$$

where M is the mass matrix, D is the viscous damping matrix, K is the stiffness matrix, f_m is the external loading vector and f_e is the generalized control force vector produced by electromechanical coupling effects. The independent variable vector $q(t)$ is composed of transversal deflections ω_i and rotations ψ_i, i.e.,[4]

$$q(t) = \begin{bmatrix} \omega_1 \\ \psi_1 \\ \vdots \\ \omega_n \\ \psi_n \end{bmatrix} \tag{14}$$

where n is the number of nodes used in the analysis. Vectors w and f_m are positive upwards. For the state-space control transformation,we are presented with,

$$\dot{x}(t) = \begin{bmatrix} q(t) \\ \dot{q}(t) \end{bmatrix} \tag{15}$$

Furthermore to express $f_e(t)$ in the form of $Bu(t)$ we write it as the product $f_e^* u$, where f_e^* is the piezoelectric force for a unit applied on the corresponding actuator, and u represents the voltages on the actuators. Finally, $d(t) = f_m(t)$ is the disturbance vector[3]. Then,

$$\dot{x}(t) = \begin{bmatrix} 0_{2n\times 2n} & I_{2n\times 2n} \\ -M^{-1}K & -M^{-1}D \end{bmatrix} x(t) + \begin{bmatrix} 0_{2n\times n} \\ M^{-1}f_e^* \end{bmatrix} u(t) + \begin{bmatrix} 0_{2n\times 2n} \\ M^{-1} \end{bmatrix} \tag{16}$$

$$= Ax(t) + Bu(t) + Gd(t) = Ax(t) + \begin{bmatrix} B & G \end{bmatrix} \begin{bmatrix} u(t) \\ d(t) \end{bmatrix} = Ax(t) + \tilde{B}\tilde{u}(t) \tag{17}$$

The previous description of the dynamical system will be augmented with the output equation (*displacements* only measured)[5],

$$y(t) = [x_1(t) \quad x_3(t) \quad \dots \quad x_{n-1}(t)]^T = Cx(t) \tag{18}$$

In this formulation u is $n \times 1$ (at most, but can be smaller), while d is $2n \times 1$. The units used are compatible for instance m, rad, sec and N. [6, 8]

3 DESIGN OBJECTIVES AND SYSTEM SPECIFICATIONS

The structured singular value of the transfer function to what matrix is defined as,

$$\mu(M) = \begin{cases} \frac{1}{\min_{k_m}\{det(I-k_m M\Delta)=0,\, \bar{\sigma}(\Delta)\leq 1\}} \\ 0,\ \Delta\ det(I - M\Delta) = 0 \end{cases} \tag{19}$$

This quantity defines the smallest structured $\mu(M)$(measured in terms of $\bar{\sigma}(\Delta)$)which makes $det(I - M\Delta) = 0$: then $\mu(M) = \frac{1}{\bar{\sigma}(\Delta)}$. It follows that values of μ smaller than 1 are desired [12, 13]

The design objectives fall into two categories:

1. Stability of closed loop system (plant+controller).
   (a) Disturbance attenuation with satisfactory transient characteristics (overshoot, settling time).
   (b) Small control effort.
2. Robust performance

Stability of closed loop system (plant+controller) should be satisfied in the face of modelling errors. [10]

In order to obtain the required system specifications with respect to the above objectives we need to represent our system in the so-called - Δ structure. Let us start with the simple typical diagram of Fig. 3. [14, 15]

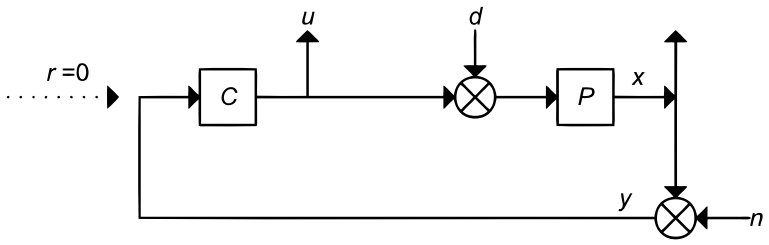

Figure 3: Classical control block diagram (P: plant dynamical system, C: controller)

In this diagram there are two inputs, d and n, and two outputs, u and x. In what follows it is assumed that,

$$\left\| \begin{matrix} d \\ n \end{matrix} \right\|_2 \leq 1, \quad \left\| \begin{matrix} x \\ u \end{matrix} \right\|_2 \leq 1 \tag{20}$$

If this is not the case, appropriate frequency-dependent weights can transform original signals so that the transformed signals have this property. The details of the system are given in Fig.4:

In this description,

$$z = \begin{bmatrix} u \\ x \end{bmatrix}, \quad w = \begin{bmatrix} d \\ n \end{bmatrix} \tag{21}$$

where z are the output variables to be controlled, and w the exogenous inputs.

Given that P has two inputs and two outputs it is, as usual, naturally partitioned as,

$$\begin{bmatrix} z(s) \\ y(s) \end{bmatrix} = \begin{bmatrix} P_{zw}(s) & P_{zu}(s) \\ P_{yw}(s) & P_{yu}(s) \end{bmatrix} \begin{bmatrix} w(s) \\ u(s) \end{bmatrix} = P(s) \begin{bmatrix} w(s) \\ u(s) \end{bmatrix} \tag{22}$$

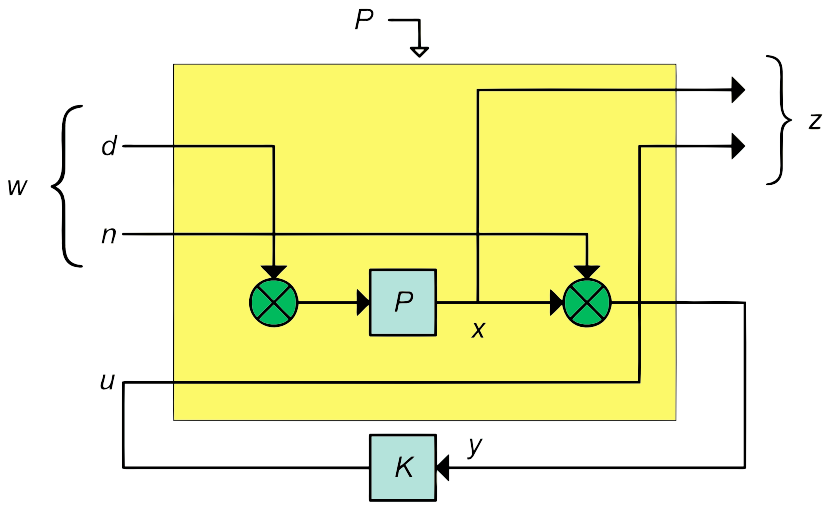

Figure 4: Detailed two-port diagram (with a linear feedback control K)

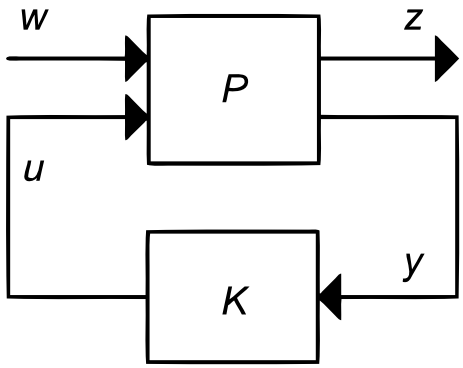

Figure 5: Two-port diagram

In addition the controller is written,

$$u(s) = K(s)y(s) \tag{23}$$

Substituting (22) in (23) gives the closed loop transfer function $N_{zw}(s)$,

$$N_{zw}(s) = P_{zw}(s) + P_{zu}(s)K(s)(I - P_{yu}(s)K(s))^{-1}P_{yw}(s) \tag{24}$$

To deduce robustness specifications one more diagram is needed, namely that of Figure 6: where N is defined by (24) and the uncertainty modelled in Δ satisfies $||\Delta||_\infty \leq 1$ (details are given later on in this paper). Here,

$$z = \mathcal{F}_u(N, \Delta)w = [N_{22} + N_{21}\Delta(I - N_{11}\Delta)^{-1}N_{12}]w = Fw \tag{25}$$

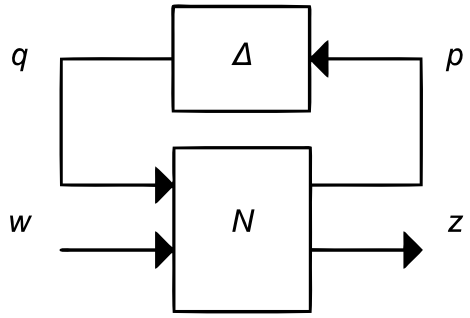

Figure 6: Two port diagram with uncertainty

Given this structure we can state the following definitions:

$$\begin{gathered}\text{Nominal stability } (NS) \Leftrightarrow N \text{ internally stable} \\ \text{Nominal performance } (NP) \Leftrightarrow ||N_{22}(j\omega)||_\infty \leq 1 \ \forall\omega \text{ and } NS \\ \text{Robust stability } (RS) \Leftrightarrow F = \mathcal{F}_u(N,\Delta) \text{ stable } \forall\Delta,\ ||\Delta||_\infty < 1 \text{ and } NS \\ \text{Robust performance } (RP) \Leftrightarrow ||F||_\infty < 1,\ \forall\Delta,\ ||\Delta||_\infty < 1 \text{ and } S\end{gathered} \tag{26}$$

It has been proved that the following conditions hold in the case of block-diagonal real or complex perturbations Δ:

1. The system is nominally stable if M is internally stable.
2. The system exhibits nominal performance if $\bar{\sigma}(N_{22}(j\omega)) < 1$
3. The system (M, Δ) is robustly stable if and only if,

$$\sup_{\omega\in\mathbb{R}} \mu_\Delta(N_{11}(j\omega)) < 1 \tag{27}$$

   where μ_Δ is the structured singular value of N given the structured uncertainty set Δ. This condition is known as the generalized small gain theorem.

4. The system (N, Δ) exhibits robust performance if and only if,

$$\sup_{\omega\in\mathbb{R}} \mu_{\Delta_a}(N(j\omega)) < 1 \tag{28}$$

   where,

$$\Delta_a = \begin{bmatrix}\Delta_p & 0 \\ 0 & \Delta\end{bmatrix} \tag{29}$$

   and Δ_p is full complex, has the same structure as Δ and dimensions corresponding to w, z. [15]
   Unfortunately, only bounds on μ can be estimated.

3.1 Controller synthesis

All the above results support the analysis problem and provide tools to judge the performance of any controller or to compare different controllers. However it is possible to approximately synthesize a controller that achieves given performance in terms of the structured singular value μ.

In this procedure, which is called $(D, G-K)$ iteration [20] the problem of finding an μ-optimal controller K such that $\mu(\mathcal{F}_u(F(j\omega)), K(j\omega)) \leq \beta, \forall\omega$ is transformed into the problem of finding transfer function matrices $D(\omega) \in \mathcal{D}$ and $G(\omega) \in \mathcal{G}$, such that,

$$\sup_{\omega} \bar{\sigma} \left[\left(\frac{D(\omega)\mathcal{F}_u(F(j\omega), K(j\omega))D^{-1}(\omega)}{\gamma} - jG(\omega) \right) \left(I + G^2(\omega)\right)^{-\frac{1}{2}} \right] \leq 1, \quad \forall\omega \tag{30}$$

Unfortunately this method does not guarantee even finding local maxima. However for complex perturbations a method known as $D-K$ iteration is available (implemented in MATLAB). [20] It combines H_∞ synthesis and μ-analysis and often yields good results. The starting point is an upper bound on μ in terms of the scaled singular value,

$$\mu(N) \leq \min_{D\in\mathcal{D}} \bar{\sigma}(DND^{-1}) \tag{31}$$

The idea is to find the controller that minimizes the peak over the frequency range namely,

$$\min_{K} \left(\min_{D\in\mathcal{D}} ||DN(K)D^{-1}||_\infty \right) \tag{32}$$

by alternating between minimizing $||DN(|K)D^{-1}||_\infty$ with respect to either K or D (while holding the other fixed).

1. **K-step**. Synthesize an $\mathcal{H}_\infty$ controller for the scaled problem $\min_K ||DN(K)D^{-1}||_\infty$ with fixed $D(s)$.
2. **D-step**. Find $D(j\omega)$ to minimize at each frequency $\bar{\sigma}(DND^{-1}(j\omega))$ with fixed N.
3. Fit the magnitude of each element of $D(j\omega)$ to a stable and minimum phase transfer function $D(s)$ and got to Step 1. [20]

3.2 System uncertainty

Let us assume uncertainty in the mass M and K matrices of the form,

$$\begin{aligned} K &= K_0(I + k_p I_{2n\times 2n}\delta_K) \\ M &= M_0(I + m_p I_{2n\times 2n}\delta_M) \end{aligned} \tag{33}$$

Alternatively, since in general the Reyleigh damping assupmtion is,

$$D = aK + \beta M \tag{34}$$

D could be expressed similarly to K, M, as,

$$D = D_0(I + d_p I_{2n\times 2n}\delta_D) \tag{35}$$

In this way we introduce uncertainty in the form of percentage variation in the relevant matrices. More detailed correlation of uncertainty with certain properties of the structures (e.g., material constants, flexibility of joints, cracks or delaminations) is possible and will be investigated in the future.

Here it will be assumed,

$$||\Delta||_\infty \stackrel{def}{=} \left\| \left[\begin{array}{c|c} I_{n\times n}\delta_K & 0_{n\times n} \\ \hline 0_{n\times n} & I_{n\times n}\delta_M \end{array}\right] \right\|_\infty < 1 \tag{36}$$

hence m_p, k_p are used to scale the percentage value and the zero subscript denotes nominal values (it is reminded here that the norm for a matrix $A_{n\times n}$ is calculated through $||A||_\infty = \max_{1\le j\le m}\sum_{j=1}^{n}|a_{ij}|$)

With these definitions Eq. 13 becomes,

$$\begin{gathered} M_0(I + m_p I_{2n\times 2n}\delta_M)\ddot{\boldsymbol{w}}(t) + K_0(I + k_p I_{2n\times 2n}\delta_K)\boldsymbol{w}(t) \\ +[D_0 + 0.0005[K_0 k_p I_{2n\times 2n}\delta_K + M_0 m_p I_{2n\times 2n}\delta_M]]\dot{w}(t) = f_m(t) + f_e(t) \\ \Rightarrow M_0\ddot{\boldsymbol{w}}(t) + D_0\dot{q}(t) + K_0\boldsymbol{w}(t) = \\ -[M_0 m_p I_{2n\times 2n}\delta_M\ddot{\boldsymbol{w}}(t) + 0.0005[K_0 k_p I_{2n\times 2n}\delta_K + M_0 m_p I_{2n\times 2n}\delta_M]\dot{\boldsymbol{w}}(t) + \\ K_0 k_p I_{2n\times 2n}\delta_K \boldsymbol{w}(t)] \\ = f_m(t) + f_e(t) \\ \Rightarrow M_0\ddot{\boldsymbol{w}}(t) + D_0\dot{\boldsymbol{w}}(t) + K_0\boldsymbol{w}(t) = \tilde{D}q_u(t) + f_m(t) + f_e(t) \end{gathered} \tag{37}$$

where,

$$q_u(t) = \begin{bmatrix} \ddot{\boldsymbol{w}}(t) \\ \dot{\boldsymbol{w}}(t) \\ \boldsymbol{w}(t) \end{bmatrix} \tag{38}$$

$$\begin{aligned} \tilde{D} &= -\begin{bmatrix} M_0 m_p & K_0 k_p \end{bmatrix} \left[\begin{array}{c|c} I_{2n\times 2n}\delta_M & 0_{2n\times 2n} \\ \hline 0_{2n\times 2n} & I_{2n\times 2n}\delta_K \end{array}\right] \begin{bmatrix} I_{2n\times 2n} & 0.0005 I_{2n\times 2n} & 0_{2n\times 2n} \\ 0_{2n\times 2n} & 0.0005 I_{2n\times 2n} & I_{2n\times 2n} \end{bmatrix} \\ &= G_1 \cdot \Delta \cdot G_2 \end{aligned} \tag{39}$$

Writing (37) in state space form, gives,

$$\begin{aligned} \dot{x}(t) &= \begin{bmatrix} 0_{2n\times 2n} & I_{2n\times 2n} \\ -M^{-1}K & -M^{-1}D \end{bmatrix} x(t) + \begin{bmatrix} 0_{2n\times 2n} \\ M^{-1}f_e^* \end{bmatrix} u(t) + \begin{bmatrix} 0_{2n\times 2n} \\ M^{-1} \end{bmatrix} d(t) + \begin{bmatrix} 0_{2n\times 6n} \\ M^{-1}F_1 \cdot \Delta \cdot G_2 \end{bmatrix} q_u(t) \\ &= Ax(t) + Bu(t) + Gd(t) + G_u G_2 q_u(t) \end{aligned} \tag{40}$$

In this way we treat uncertainty in the original matrices as an extra uncertainty term. To express our system in the form of Fig. 6, consider Fig. 7.

The matrices E_1, E_2 are used to extract,

$$q_u(t) \stackrel{def}{=} \begin{bmatrix} \ddot{\boldsymbol{w}}(t) \\ \dot{\boldsymbol{w}}(t) \\ \boldsymbol{w}(t) \end{bmatrix} \tag{41}$$

Since,

$$\gamma = \begin{bmatrix} \dot{\boldsymbol{w}}(t) \\ \ddot{\boldsymbol{w}}(t) \end{bmatrix} \qquad \beta = \int \begin{bmatrix} \dot{\boldsymbol{w}}(t) \\ \ddot{\boldsymbol{w}}(t) \end{bmatrix} dt = \begin{bmatrix} \boldsymbol{w}(t) \\ \dot{\boldsymbol{w}}(t) \end{bmatrix} \tag{42}$$

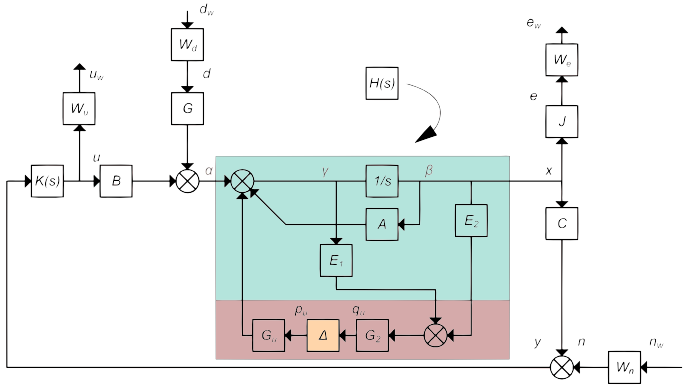

Figure 7: Uncertainty block diagram.

appropriate choices for E_1, E_2 are,

$$E_1 = \begin{bmatrix} 0_{2n\times 2n} & \vdots & I_{2n\times 2n} \\ \cdots & \vdots & \cdots \\ I_{2n\times 2n} & \vdots & 0_{2n\times 2n} \\ \cdots & \vdots & \cdots \\ 0_{2n\times 2n} & \vdots & 0_{2n\times 2n} \end{bmatrix}, \quad E_2 = \begin{bmatrix} 0_{2n\times 2n} & \vdots & 0_{2n\times 2n} \\ \cdots & \vdots & \cdots \\ 0_{2n\times 2n} & \vdots & 0_{2n\times 2n} \\ \cdots & \vdots & \cdots \\ I_{2n\times 2n} & \vdots & 0_{2n\times 2n} \end{bmatrix} \tag{43}$$

The idea is to find an N such that,

$$\begin{bmatrix} q_u \\ \cdots \\ e_w \\ u_w \end{bmatrix} = N \begin{bmatrix} p_u \\ \cdots \\ d_w \\ n_w \end{bmatrix}, \quad N = \begin{bmatrix} N_{p_u q_u} & \vdots & N_{d_w q_u} & N_{n_w q_u} \\ \cdots & \vdots & \cdots & \cdots \\ N_{p_u e_w} & \vdots & N_{d_w e_w} & N_{n_w e_w} \\ N_{p_u u_w} & \vdots & N_{d_w u_w} & N_{n_w u_w} \end{bmatrix} = \begin{bmatrix} N_{11} & N_{12} \\ N_{21} & N_{22} \end{bmatrix} \tag{44}$$

or in the notation of Fig. 6

$$\begin{bmatrix} q_u \\ \boldsymbol{w} \end{bmatrix} = N \begin{bmatrix} p_u \\ z \end{bmatrix} \tag{45}$$

Now $N_{d_w e_w}$, $N_{n_w e_w}$, $N_{n_w u_w}$ are known. For the rest we will use a methodology known as "pulling out the Δ's". To this end, break the loop at points p_u, q_u (which will be used as additional inputs/outputs respectively) and use the auxiliary signals a, β, γ. To get the transfer function $N_{d_w q_u}$ (from d_w to q_u):

$$q_u = G_2(E_2\beta + E_1\gamma) = G_2(E_2\frac{1}{s} + E_1)\gamma \tag{46}$$

$$\gamma = GW_d d_w + Bu + A\frac{1}{s}\gamma = GW_d d_w + BKC\frac{1}{s}\gamma + A\frac{1}{s}\gamma \tag{47}$$

$$\Rightarrow \gamma = (I - BKC\frac{1}{s} - A\frac{1}{s})^{-1} GW_d d_w \tag{48}$$

Hence,

$$N_{d_w q_u} = G_2(E_2\frac{1}{s} + E_1)(I - BKC\frac{1}{s} - A\frac{1}{s})^{-1}GW_d \tag{49}$$

Now, $N_{p_u q_u}$, $N_{p_u e_w}$, $N_{p_u u_w}$, are similar to $N_{d_w q_u}$, $N_{d_w e_w}$, $N_{d_w u_w}$, with GW_d replaced by G_u, i.e.,

$$\begin{aligned} N_{p_u q_u} &= G_2(E_2\frac{1}{s} + E_1)(I - BKC\frac{1}{s} - A\frac{1}{s})^{-1}G_u \\ N_{p_u e_w} &= W_y JH[I + B[K(I - CHBK)^{-1}CH]]G_u \\ M_{p_u u_w} &= W_u K(I - CHBK)^{-1}CHG_u \end{aligned} \tag{50}$$

Finally to find $N_{n_w q_u}$,

$$q_u = G_2(E_2\beta + E_1\gamma) = G_2(E_2\frac{1}{s} + E_1)\gamma \tag{51}$$

$$\gamma = Bu + A\frac{1}{s}\gamma = BK(W_n n_w + y) + A\frac{1}{s}\gamma = BKW_n n_w + BKC\frac{1}{s}\gamma + A\frac{1}{s}\gamma \tag{52}$$

$$\Rightarrow \gamma = (I - BKC\frac{1}{s} - A\frac{1}{s})^{-1}BKW_n n_w \tag{53}$$

Hence,

$$N_{n_w q_u} = G_2(E_2\frac{1}{+}E_1)(I - BKC\frac{1}{s} - A\frac{1}{s})^{-1}BKW_n \tag{54}$$

Collecting all the above yields N:

$$N = \begin{bmatrix} G_2\left(E_2\frac{1}{s}+E_1\right)\left(I-BKC\frac{1}{s}-A\frac{1}{s}\right)^{-1}G_u & G_2\left(E_2\frac{1}{s}+E_1\right)\left(I-BKC\frac{1}{s}-A\frac{1}{s}\right)^{-1}GW_d & G_2\left(E_2\frac{1}{s}+E_1\right)\left(I-BKC\frac{1}{s}-A\frac{1}{s}\right)^{-1}BKW_u \\ W_e JH\left[I+BK(I-CHBK)^{-1}CF\right]G_u & W_e J(I-HBKC)^{-1}HGW_d & W_e J(I-HBKC)^{-1}HBKW_u \\ W_u K(I-CHBK)^{-1}CFG_u & W_u(I-KCHB)^{-1}KCHGW_d & W_u(I-KCHB)^{-1}KW \end{bmatrix} \tag{55}$$

Having obtained N for the beam problem, all proposed controllers $K(s)$ can be compared using the structured singular value relations. [18, 19, 21]

4 ROBUSTNESS ISSUES

The superiority of H_∞ control lies in its ability to take explicitly into account the worst effect of unknown disturbances and noise in the system. Furthermore, at least in theory, it is possible to synthesize an H_∞ controller that is robust to a prescribed amount of modeling errors. Unfortunately, this last possibility is not implementable in some cases, as it will be subsequently illustrated.[16, 17]

In what follows, the robustness to modeling errors of the designed H_∞ controller will be analyzed. Furthermore an attempt to synthesize a μ-controller will be presented, and comparisons between the two will be made.

In all simulations, routines from Matlab's Robust Control Toolbox will be used. In particular:

1. For uncertain elements,

2. To calculate bounds on the structured singular value,

3. To calculate a μ-controller,

Numerical models used in all simulations, are implemented in three ways:

1. Through Eq. 56

$$\begin{aligned} K &= K_0(I + k_p I_{2n\times 2n}\delta_K) \\ M &= M_0(I + m_p I_{2n\times 2n}\delta_M) \\ D &= D_0 + 0,0005[K_0 k_p I_{2n\times 2n}\delta_K + M_0 m_p I_{2n\times 2n}\delta_M] \end{aligned} \tag{56}$$

   and subsequent evaluation of matrix N for specific values of k_p, m_p.

2. By use of Matlab's "uncertain element object". As explained, this form is needed in the D-K robust synthesis algorithm.

3. By Simulink implementation of Fig. 8.

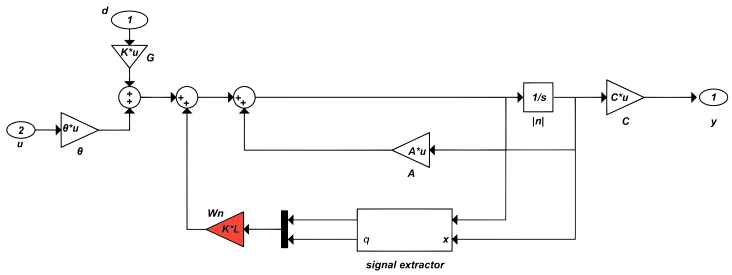

Figure 8: Simulink diagram of uncertain plant

4.1 Robust analysis - Results

Robust analysis is carried out through the relations:

$$\sup_{\omega\in\mathbb{R}} \mu_{\Delta}(N_{11}(j\omega)) < 1 \tag{57}$$

for robust stability, and,

$$\sup_{\omega\in\mathbb{R}} \mu_{\Delta_a}(N(j\omega)) < 1 \tag{58}$$

for robust performance.

In all the simulations that follow the disturbance is the mechanical load, i.e. $10N$ at the free end. For the H_∞ found, robust analysis was performed for the following values of m_p, k_p.

1. $m_p = 0$, $k_p = 0.9$. This corresponds to a $\pm 90\%$ variation from the nominal value of the stiffness matrix K.

   In Fig. 9 the displacement responses for this controller for the mechanical input are shown. In Fig. 10 are shown the bounds on the μ values. As seen the system remains

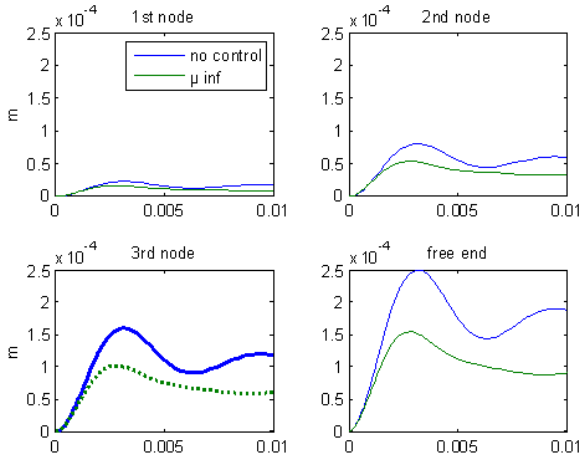

Figure 9: Displacement response loading equal to 10N at free end, μ-controller for $m_p = 0$, $k_p = 0.9$

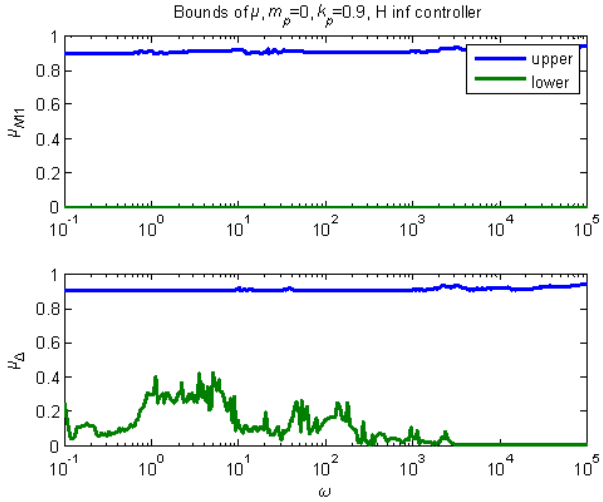

Figure 10: μ-bounds of the H_∞ controller for $m_p = 0$, $k_p = 0.9$

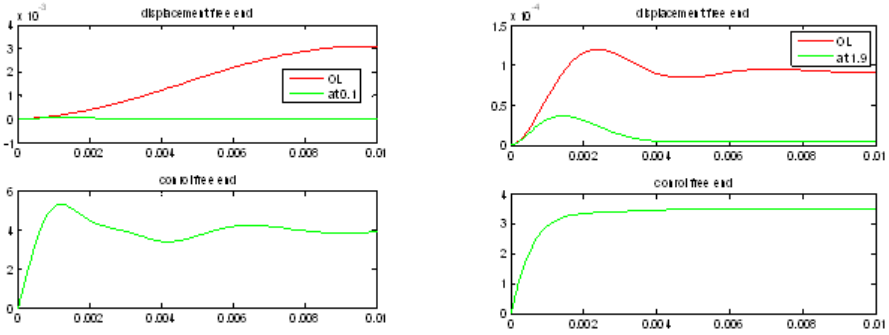

Figure 11: Displacement and control at free end for the H_∞ controller with $m_p = 0$, $k_p = 0.9$ (extreme values)

stable and exhibits robust performance, since the upper bounds of both values remain below 1 for all frequencies of interest. This result is validated in Fig. 11, where the displacement of the free end and the voltage applied are shown at the extreme uncertainty. Comparison with the open loop response for the same plant shows the good performance of the nominal controller.

2. $m_p = 0.9$, $k_p = 0$. This corresponds to a $\pm 90\%$ variation from the nominal value of the mass matrix M.

   In Fig. 12 are shown the bounds on the μ values. As seen the system remains stable and exhibits robust performance, since the upper bounds of both values remain below 1 for all frequencies of interest. This result is validated in Fig. 13, where the displacement of the free end and the voltage applied are shown. Comparison with the open loop response for the same plant shows the good performance of the nominal controller.

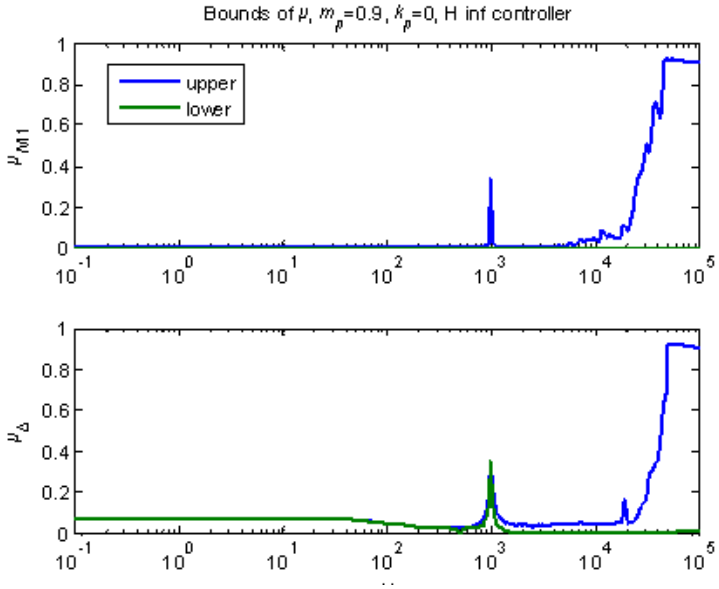

Figure 12: μ-bounds of the H_∞ controller for $m_p = 0.9$, $k_p = 0$

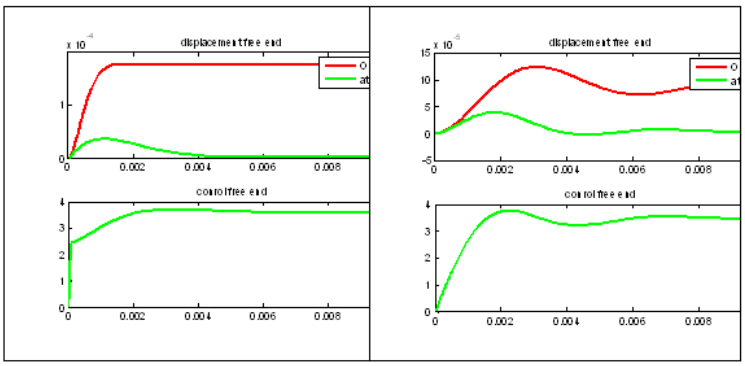

Figure 13: Displacement and control at free end for the H_∞ controller with $m_p = 0.9$, $k_p = 0$(extreme values)

3. $m_p = 0.9$, $k_p = 0.9$. This corresponds to a $\pm 90\%$ variation from the nominal values of both the mass and stiffness matrices M, K.

   In Fig. 14 are shown the bounds on the μ values. As seen the system remains stable and exhibits robust performance, since the upper bounds of both values remain below 1 for all frequencies of interest. This result is validated in Fig. 15, where the displacement of the free end and the voltage applied are shown. Comparison with the open loop response for the same plant shows the good performance of the nominal controller.

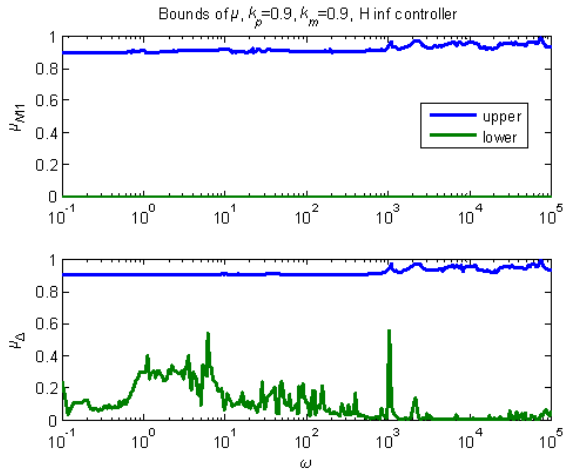

Figure 14: Displacement and control at free end for the H_∞ controller with $m_p = 0.9$, $k_p = 0$(extreme values)

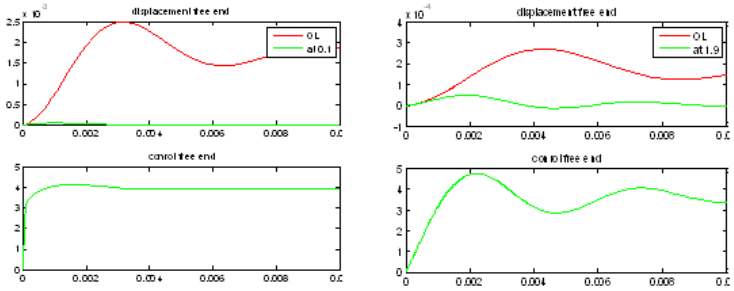

Figure 15: Displacement and control at free end for the H_∞ controller with $m_p = 0.9$, $k_p = 0$(extreme values)

5 CONCLUSIONS

In this paper advanced control techniques, like criterion H_∞ and m-analysis, have been applied for the suppression vibrations of smart structures. Under the assumption of an uncertainty introduced at the level of matrices in the structural analysis of the system the robust characteristics of the H_∞ controller and m-analysis were checked. There was a complete suppression of the oscillation and rigidity of the beam up to and including 90% variation from the nominal values.

An effort was made to find a robust μ-controller, using the recurring method $D - K$. In this case the resulting order of the controller as well as the required calculation requirements was very large. The performance of the robust μ-controller was not the one expected, something that most likely is due to the numerical properties of the system tables. Contrary to the H_∞ controller, the results are quite satisfactory and prove that the H_∞ control can suppress the oscillation of the smart beam taking into account the modelling uncertainties, external disturbances and the noise of the measurements.

In summary, the scientific fields which this paper has contributed to are:

- Application of the control in suppressing the oscillation of structural models.
- Introduction of the uncertainties in the mathematic model of structural elements.
- Suppression of oscillation and rejection of disturbances, by taking into account the modelling error, using the criterion of the robust H_∞ control.

- Reduction of the calculation requirements of the control using optimisation algorithms.
- Finding of a robust μ-controller

Experimental verification of the very good results that were found in this work as well as further detailed correlation of uncertainties with the real parameters of the mechanical system (material parameters, joints, cracks and delaminations etc) remain open for future investigations.

REFERENCES

[1] J. Friedman, K. Kosmatka, *An improved two node Timoshenko beam finite element*, Computer and Structures, vol. 47, pp. 473-481, 1993.

[2] G. Foutsitzi, D. Marinova, E. Hadjigeorgiou and G. Stavroulakis, *Robust H2 vibration control of beams with piezoelectric sensors and actuators*, Proceedings of Physics and Control Conference (PhyCon03), St. Petersburg, Russia, 20-22 August, Vol. I, pp. 158-163, 2003.

[3] C. Sisemore, A. Smaili, R. Houghton, *Passive damping of flexible mechanism system: experimental and finite element investigation*, The 10^{th} World Congress of the Theory of Machines and Mechanisms, Oulu, Finland, Vol. 5, pp. 2140-2145, 1999.

[4] N. Zhang, I. Kirpitchenko, *Modelling dynamics of a continuous structure with a piezoelectric sensor/actuator for passive structural control*, Journal of Sound and Vibration, vol. 249, pp. 251-261, 2002.

[5] B. Miara, G. Stavroulakis, V. Valente (Eds.), *Topics on mathematics for smart systems*. Proceedings of the European Conference, Rome, Italy, 26-28 October 2006, World Scientific Publishers, Singapore, International, 2007.

[6] B. Shahian, M. Hassul, *Control system design using MATLAB*, Prentice-Hall, NJ, 1994.

[7] W.S. Huang, H.C. Park, *Finite element modelling of piezoelectric sensors and actuators*, American Institute of Aeronautics and Astronautics Journal, vol.31, pp. 930-937, 1993.

[8] G. Foutsitzi, D. Marinova, E. Hadjigeorgiou, G. Stavroulakis, *Finite element modelling of optimally controlled smart beams*, 28Ih Summer School: *Applications of Mathematics in Engineering and Economics*, Sozopol, Bulgaria, 2002.

[9] G.E. Stavroulakis, G. Foutsitzi, E. Hadjigeorgiou, D. Marinova, C.C. Baniotopoulos, *Design and robust optimal control of smart beams with application on vibrations suppression* Advances in Engineering Software, Volume 36, Issues 11-12, Pages 806-813, November-December 2005.

[10] J.V. Burke, D. Henrion, M.L. Lewis, *Overton.HIFOO-a MATLABpackage for fixed-order controller design and Hinf. optimization.* Proceedings of the IFAC Symbosium on Robust Control Design, Toulouse, France, 2006. www.cs.nyu.edu/overton/software/hifoo

[11] H.F. Tiersten, *Linear Piezoelectric Plate Vibrations*, Plenum Press New York, 1969.

[12] J.V. Burke, D. Henron, A.S. Kewis and M.L. Overton, *Stabilization via Nonsmooth, Nonconvex Optimization*, Automatic Control IEE Volume 5 Issue11 page1760-1769 November 2006.

[13] O. Bosgra, H. Kwakernaak, *Design methods for control systems*, Course notes, Dutch Institute for Systems and Control, p.69, 2001.

[14] M. Hou and P.C. Muller, *Design of observers for linear systems with unknown inputs*, IEEE Trans. on Automatic Control, 37: 871-875, 1992.

[15] A. Packard, J. Doyle, and G. Balas, *Linear, multivariable robust control with a perspective,* ASME Journal of Dynamic Systems, Measurement and Control, 50th Anniversary Issue, Vol. 115, no. 2b, p. 310-319, 1993.

[16] A. Pouliezos (2008). *MIMO control systems*, class notes. http://pouliezos.dpem.tuc.gr

[17] D. Marinova, G.E. Stavroulakis, D. Foutsitzi, E. Hadjigeorgiou, and E.C. Zacharenakis, *Robust design of smart structures taking into account structural defects*, Summer School Conference Advanced Problems in Mechanics Russian Academy of Sciences, Editor: D.A. Indeitsev, 288-292, 2004.

[18] A.L. Tits and Y. Yang, *Globally convergent algorithms for robust pole assignment by state feedback*, IEEE Trans. on Automatic Control, 41: 1432-1452, 1996.

[19] R.C. Ward, *Balancing the generalized eigenvalue problem*, SIAM J. Sci. Stat. Comput., 2: 141-152, 1981.

[20] P. Young, M. Newlin, and J. Doyle, *Practical computation of the mixed problem,* Proceedings of the American Control Conference, pp. 2190-2194, 1992.

[21] K.G. Arvanitis, E.C. Zacharenakis, A.G. Soldatos and G.E. Stavroulakis, *New trends in optimal structural control*, Selected Topics in Structronic and Mechatronic System, World Scientific Publishers 321-415 chapter 8, Singapore, 2003.